Supplementary Material

A Molecular Electron Density Theory Study of the [3+2] Cycloaddition Reaction of Nitrones with Ketenes

Mar Ríos-Gutiérrez,[a] Andrea Darù,[b] Tomás Tejero,[b] Luis R. Domingo*[a] and Pedro Merino*[b]

[a] Department of Organic Chemistry, University of Valencia, Dr. Moliner 50, E-46100 Burjassot, Valencia, Spain.

[b] Laboratorio de Síntesis Asimétrica, Instituto de Síntesis Química y Catálisis Homogénea (ISQCH), Universidad de Zaragoza-CSIC, Zaragoza 50009, Spain.

e-mail: domingo@utopia.uv.es; pmerino@unizar.es
web: www.luisrdomingo.com

Index

*1. BET characterisation of the molecular mechanism of the zw-type 32CA reaction between nitrone **1b** and ketene **4b**.*

When trying to achieve a better understanding of bonding changes in organic chemical reactions, the so-called Bonding Evolution Theory[1] (BET) has proved to be a very useful methodological tool.[2] BET applies Thom's catastrophe theory[3] (CT) concepts to the topological analysis of the gradient field of the Electron Localisation Function[4] (ELF) along the reaction coordinate. Several theoretical studies have shown that the topological analysis of the ELF offers a suitable framework for the study of the changes of electron density. This methodological approach is used as a valuable tool to understand the bonding changes along the reaction path and, consequently, to establish the nature of the electronic rearrangement associated with a given molecular mechanism.[5]

Recently, a BET study of the bonding changes along the *zw-type* 32CA reactions of nitrone **1a** with electron deficient acrolein **13** was carried out in order to understand the O–C and C–C bond formation processes and to know the molecular mechanism of these *zw-type* 32CA processes.[6] On the other hand, a recent BET study of the molecular mechanism of the ketene-imine Staudinger reaction[7] permitted to characterise the participation of the C–C double bond of the ketene in the second step of this reaction. Herein, in order to understand the participation of the O–C double bond of ketenes, a BET study of the most favourable reaction channel associated with the 32CA reaction between nitrone **1b** and ketene **4b** is performed with the aim of characterising the molecular mechanism of 32CA reactions involving ketenes.

BET study of the most favourable reactive channel associated with the 32CA reaction between nitrone **1b** and ketene **4b** indicates that it takes place along eight differentiated phases related to the disappearance or creation of valence basins. A representation of the relative energy of the bonding changes and the GEDT process computed by an NPA along the reaction channel is given in Figure S1; the eight phases in which the reaction path is topologically divided are separated by black hyphened lines crossing the energy curve. The populations of the most significant valence basins (those associated with the bonding regions and lone pairs directly involved in the reaction) of the selected points of the IRC are included in Table S1, the attractor positions of the ELF basins for the points involved in the bond formation processes are shown in Figure S2 and the basin-population changes along the reaction path are

graphically represented in Figure S3. Finally, the equivalence between the topological features of the selected points and the associated chemical changes are given in Table S2.

The long *Phase I* (see Figure S1), 3.05 Å ≥ d(O1−C5) > 2.28 Å and 3.26 Å ≥ d(C3−O4) > 2.76 Å, begins at **MC-b**, which is a minimum in the PES connecting the separated reagents, nitrone **1b** and ketene **4b**, with **TS-CO**. The ELF picture of **MC-b** shows the topological features of the separated reagents. Thus, the two monosynaptic basins, V(O1) and V'(O1), integrating a total population of 5.99e, are associated with the two O1 oxygen lone pairs of the nitrone framework. While the V(O1,N2) disynaptic basin with a low electron population of 1.48e describes the O1−N2 bonding region, the two V(N2,C3) and V'(N2,C3) disynaptic basins, integrating a total of 3.79e, depict the N2−C3 double bond of the nitrone framework. On the other hand, the two monosynaptic basins, V(O4) and V'(O4), integrating a total of 4.93e, are associated with the two O4 oxygen lone pairs of the ketene framework, while the two disynaptic basins V(O4,C5) and V'(O4,C5), with a total of 2.70e, depict the O4−C5 bonding region. Interestingly, the low electron density in the O1−N2 bonding region and the very high population of the O1 oxygen lone pairs indicates that the O1−N2 single bond is considerably polarised towards the O1 oxygen atom. At **MC-b**, the GEDT is null, 0.01e.

Phase II, 2.28 Å ≥ d(O1−C5) > 1.80 Å and 2.76 Å ≥ d(C3−O4) > 2.55 Å, begins at **P1**, which is identified by means of a *C* cusp catastrophe. At this point, the two V(O4,C5) and V'(O4,C5) disynaptic basins present at **MC-b** have merged into a new V(O4,C5) disynaptic basin, integrating 2.52e, as a consequence of the depopulation of the O4−C5 bonding region by 0.18e. This electron density is gathered at the V(O4) and V'(O4) monosynaptic basins, whose populations increase to a total of 5.12e. At the nitrone interacting framework, no significant electron density changes are observed (see Table S1). The GEDT at **P1** has slightly increased to 0.09e.

The very short *Phase III* (see Figure S1), 1.80 Å ≥ d(O1−C5) > 1.79 Å and 2.55 Å ≥ d(C3−O4) > 2.54 Å, begins at **P2**, which corresponds to a coupled *CF* cusp and fold catastrophes. At this point, the electron density in the N2−C3 bonding region of the nitrone framework has been redistributed in such a manner that it is now characterised by the presence of only one V(N2,C3) disynaptic basin (*C* cusp catastrophe), proceeding from the merger of the two predecessor, although its population is exactly

the same as in previous points (see Table S1). At the same time, while the V(O4,C5) disynaptic basin continues its depopulation to 2.32e, and thereby the population of the V(O4) and V'(O4) monosynaptic basins slightly increases, a new V(C5) monosynaptic basin is created at the C5 carbon of the ketene moiety (*F* fold catastrophe) with a very low electron population of 0.02e, this meaningless population being maintained until the end of *phase III*. Similarly, the population of the V(O1,N2) disynaptic basin slightly decreases while that of the V(O1) and V'(O1) monosynaptic ones slightly increases. At **P2**, the GEDT has strongly increased to 0.28e, a value consistent with the high polar character of the reaction.

Phase IV, 1.79 Å $\geq$ d(O1−C5) > 1.64 Å and 2.54 Å $\geq$ d(C3−O4) > 2.39 Å, begins at **P3**. This point is characterised by a *F* fold catastrophe implying the disappearance of the V(C5) monosynaptic basin created at the previous point **P2**. Along *Phase IV*, no more significant bonding changes occur. At **P3**, the GEDT remains at the value of 0.28e.

The changes in electron density taking place along *Phases I - IV*, which are mainly associated with the depopulation of the O4−C5 bonding region and slight population of the O4 oxygen lone pairs of the ketene framework, have a low energy cost of 8.6 kcal·mol^{-1} (see Table S2).

Phase V, 1.64 Å $\geq$ d(O1−C5) > 1.61 Å and 2.39 Å $\geq$ d(C3−O4) > 2.33 Å, begins at **P4**. At this point, the first most relevant topological change along the reaction channel takes place. While the two V(O1) and V'(O1) monosynaptic basins have experienced a notable depopulation by a total of 0.79e, a new V(O1,C5) disynaptic basins has been created with an initial population of 0.87e by means of a $C^{\dagger}$ cusp catastrophe. This significant topological change indicates that the formation of the first O1−C5 single bond begins at the short O1−C5 distance of 1.64 Å by the donation of some electron density of the O1 oxygen lone pairs of the nitrone framework to the C5 carbon atom of the ketene moiety (see **P3** and **P4** in Figure S2 and the creation of V(O1,C5), in blue at **P4**, in Figure S3). Note that the O1 oxygen is the most nucleophilic center of nitrone **1b** and the C5 carbon corresponds to the most electrophilic center of ketene **4b** (see Section 3.2). At **P4**, coinciding with the formation of the first O1−C5 single bond, the GEDT has slightly increased to reach the maximum value along the reaction path, 0.34e. This high value, which is similar to that computed at **TS-CO**, accounts for the very strong polar character of this *zw-type* 32CA reaction.

The changes in electron density taking place along *Phase V*, which are mainly associated with the formation of the first O1−C5 single bond are almost isothermic, 0.4 (9.0) kcal·mol^{-1} (see Table S2).

At *Phase VI*, 1.61 Å ≥ d(O1−C5) > 1.46 Å and 2.33 Å ≥ d(C3−O4) > 1.91 Å, which begins at **P5** ($F^\dagger$ fold catastrophe), the only noticeable topological change is the appearance of a new V(N2) monosynaptic basin, associated with the N2 nitrogen lone pair present at the final product CA **9b**, with an initial population of 0.96e. This electron density comes mainly from the drastic and simultaneous depopulation of the N2−C3 bonding region at **P5**, so that the corresponding V(N2,C3) disynaptic basin acquires a population of 3.04e. Thus, according to Lewis's chemical bond model, **P5** could be associated with the rupture of the N2−C3 double bond of nitrone **1b** (see Table S2). The GEDT remains unchanged. In the middle of *phase VI*, the TS of the reaction, **TS-CO**, d(O1−C5) = 1.560 Å and d(C3−O4) = 2.219 Å, is found. The variations of the ELF valence basin populations at **TS-CO** show the evolution of the bonding changes in the progress towards next phase (see Table S1).

The changes in electron density taking place along *Phase VI*, which are mainly associated with the rupture of the N2−C3 double bond of nitrone **1b** and creation and further population of the N2 nitrogen lone pair, bring about a molecular relaxation energy of 4.2 (4.5) kcal·mol^{-1} (see Table S2).

Phase VII, 1.46 Å ≥ d(O1−C5) > 1.44 Å and 1.91 Å ≥ d(C3−O4) > 1.84 Å, begins at **P6**, being characterised by a $F^\dagger$ fold catastrophe. At this point, a new V(C3) monosynaptic basin, with a low electron population of 0.02e, has been created at the C3 carbon atom, which is involved in the subsequent C3−O4 single bond formation (see **P6** in Figure S2. The electron density of this C3 *pseudoradical* center evolves increasing to a maximum of 0.09e along *phase VII* and reaching a final population of 0.06e at the end of the phase. This small electron density comes from the strong depopulation of the V(N2,C3) disynaptic basin to 2.37e; as can be observed, the main amount of electron density lost by the N2−C3 bonding region along previous *phase VI* has been redistributed at the N2 nitrogen, whose associated V(N2) monosynaptic basin has reached 1.91e. Interestingly, the ELF topological characteristics at **P6** reveal that after the formation of the first O1−C5 single bond, the depopulation of the V(O4,C5) disynaptic basin and V(O1) and V'(O1) monosynaptic basins continues in order to

contribute to the population of the V(O1,C5) disynaptic basin, which reaches 1.31e. At **P6**, the GEDT has decreased to 0.24e.

The changes in electron density taking place along *Phase VII*, which are mainly associated with the creation of the C3 *pseudoradical* center and the population of the N2 nitrogen lone pair, imply a molecular relaxation energy of 2.8 (1.4) kcal·mol^{-1} (see Table S2).

Finally, *Phase VIII*, 1.44 Å ≥ d(O1−C5) ≥ 1.37 Å and 1.84 Å ≥ d(C3−O4) ≥ 1.42 Å, which begins at **P7** and ends at CA **9b**, d(O1−C5) = 1.367 Å and d(C3−O4) = 1.420 Å, contains the second most relevant topological change occurring along the reaction channel; together with the disappearance of the V(C3) monosynaptic basin and the considerable depopulation of the V(O4) and V'(O4) monosynaptic basins by a total of 0.49e, a new V(C3,O4) disynaptic basin related to the formation of the C3−O4 single bond has been created integrating an initial population of 0.60e. This significant topological change indicates that the formation of the second C3−O4 single bond takes place at the end of the reaction channel at a C3−O4 distance of 1.84 Å, by donation of some electron density of the O4 oxygen lone pairs to the C3 *pseudoradical* center (see **P6** and **P7** in Figure S2 and the creation of V(C3,O4), in green at **P7**, in Figure S3). Interestingly, at **P7**, the first O1−C5 single bond has reached *ca.* 89% of its final population at CA **9b**. Consequently, it can be considered that the present reaction follows a *two-stage one-step* mechanism,[8] in which the formation of the second C3−O4 single bond begins when the first O1−C5 one is practically already formed (see Figure S3). The GEDT has slightly decreased to 0.21e, but remains moderate even at the end of the reaction.

At CA **9b**, no significant topological changes with respect to the topological behaviour of **P7** are observed. It deserves to be mentioned the remarkable low electron population of the V(O1,N2) disynaptic basin of only 0.99e, while the O1 oxygen lone pairs gather 4.99e, which clearly emphasises the strong polarisation of the O1−N2 single bond towards the O1 oxygen, as shown in **MC-b**. Note, in addition, that these populations are non-consistent with the Lewis chemical bond model. At CA **9b**, the two O1−C5 and C3−O4 new single bonds have reached populations of 1.51e and 1.31e, and the GEDT has decayed to 0.10e.

The changes in electron density taking place along *phase VIII*, which are mainly associated to the formation and completion of the second C3−O4 single bond, imply a strong molecular relaxation energy of 24.0 (−22.7) kcal·mol^{-1} (see Table S2).

Table S1. Valence basin populations N calculated from the ELF of the IRC points, **P1**-**P7**, defining the eight phases characterising the molecular mechanism of the most favourable reactive channel associated with the *zw-type* 32CA reaction between nitrone **1b** and ketene **4b**. The stationary points **MC-b**, **TS-CO** and **9b** are also included. Distances are given in Å, GEDT values and electron populations in e, and relative energies in kcal·mol⁻¹.
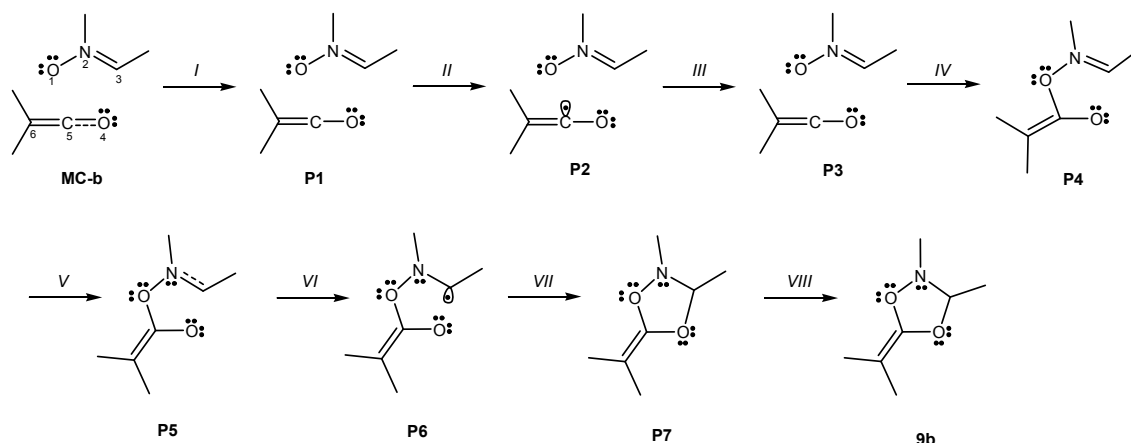
Points	MC-b	P1	P2	P3	P4	P5	P6	P7	9b	TS-CO
Catastrophes		*C*	*CF*	*F*	*C†*	*F†*	*F†*	*C†*		
Phases	*I*	*II*	*III*	*IV*	*V*	*VI*	*VII*	*VIII*		
d(O1−C5)	3.046	2.284	1.797	1.786	1.644	1.611	1.463	1.445	1.367	1.560
d(C3−C4)	3.256	2.762	2.552	2.544	2.389	2.329	1.914	1.838	1.420	2.219
ΔE	0.0	2.7	7.0	7.1	8.6	9.0	4.5	1.4	−22.7	9.3
GEDT	0.01	0.09	0.28	0.28	0.34	0.34	0.24	0.21	0.10	0.33
V(O1,N2)	1.48	1.43	1.35	1.35	1.26	1.24	1.10	1.10	0.99	1.18
V(N2)						0.96	1.91	2.01	2.35	1.31
V(N2,C3)	1.90	1.95	3.79	3.80	3.94	3.04	2.37	2.26	1.91	2.78
V'(N2,C3)	1.89	1.84								
V(O4,C5)	1.32	2.52	2.32	2.30	2.14	2.08	1.77	1.75	1.53	1.96
V'(O4,C5)	1.38									
V(C5,C6)	2.08	2.11	2.11	2.11	2.08	2.08	2.06	2.06	2.00	
V'(C5,C6)	2.09	2.11	2.08	2.07	2.03	2.01	1.96	1.97	2.05	
V(O1)	2.95	2.93	2.89	2.88	2.48	2.52	2.44	2.43	2.58	2.47
V'(O1)	3.04	3.07	3.09	3.15	2.76	2.71	2.49	2.48	2.41	2.65
V(C5)			0.02							
V(C3)							0.03			
V(O4)	2.45	2.55	2.65	2.65	3.00	3.04	2.90	2.77	2.34	3.08
V'(O4)	2.48	2.57	2.69	2.69	2.55	2.50	2.79	2.43	2.40	2.54
V(O1,C5)					0.87	0.90	1.31	1.35	1.51	1.05
V(C3,O4)								0.60	1.32	

Table S2. Sequential bonding changes along the *zw-type* 32CA reaction between nitrone **1b** and ketene **4b**, showing the equivalence between the topological characterisation of the different phases and the associated chemical process.

	Phases	d(O1−C5)	d(C3−O4)	ΔE	GEDT	Topological characterisation	Chemical process
a	*I - IV*	3.04 ≥ d > 1.79	3.26 ≥ d > 2.39	8.6	≤ 0.34	Depopulation of the V(O4,C5) disynaptic basin	Depopulation of the O4−C5 bonding region
b	*V*	1.64 ≥ d > 1.61	2.39 ≥ d > 2.33	9.0 (0.4)	0.34	Formation of the V(O1−C5) disynaptic basin	Formation of the O1−C5 single bond
c	*VI*	1.61 ≥ d > 1.46	2.33 ≥ d > 1.91	4.5 (−4.5)	≤ 0.34	Depopulation of the V(N2,C3) disynaptic basin and formation of the V(N2) monosynaptic basin	Rupture of the N2−C3 double bond and formation of the N2 nitrogen lone pair
d	*VII*	1.46 ≥ d > 1.44	1.91 ≥ d > 1.84	1.7 (−3.1)	≤ 0.24	Formation of the non-bonding V(C3) monosynaptic basin	Formation of the C3 *pseudoradical* center
e	*VIII*	1.44 ≥ d ≥ 1.37	1.84 ≥ d ≥ 1.42	−22.7 (−24.1)	≤ 0.21	Formation of the V(C3−O4) disynaptic basin	Formation of the C3−O4 single bond
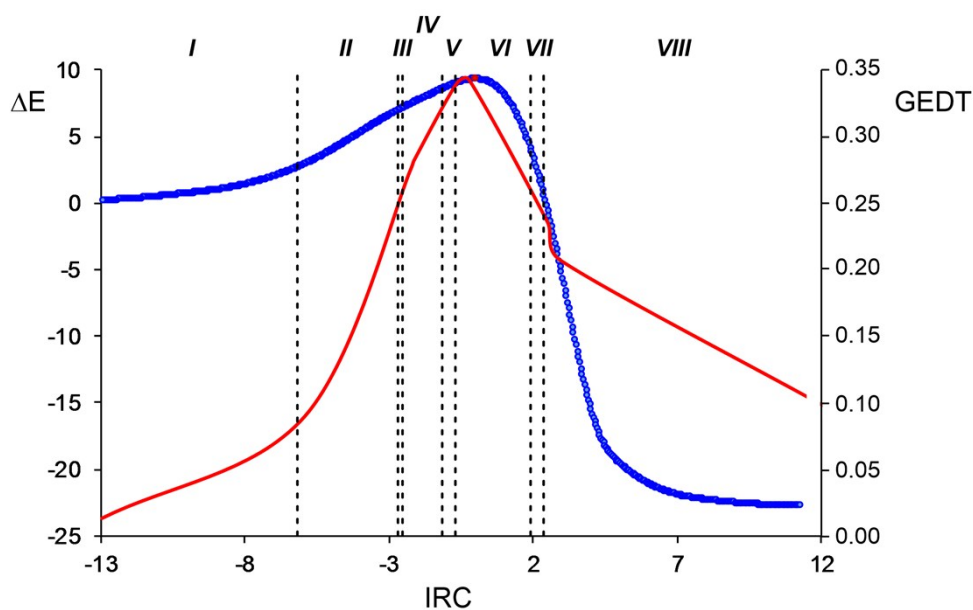
Figure S1. Relative energy (ΔE, in kcal·mol^{-1}) and GEDT (in e) variations along the IRC (amu$^{1/2}$Bohr) associated with the *zw-type* 32CA reaction between nitrone **1b** and ketene **4b** showing the relative positions of the selected points separating the topological phases along the reaction path.
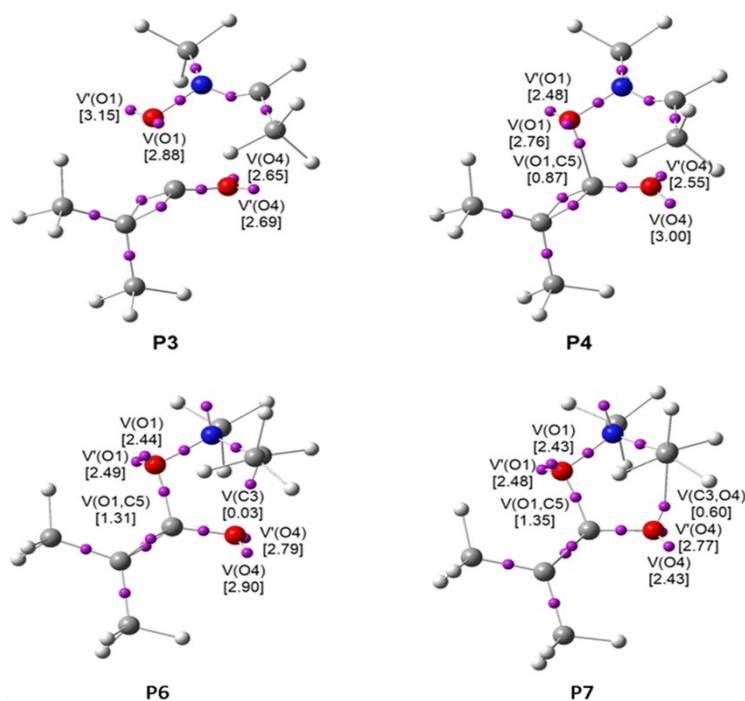

Figure S2. ELF attractor positions for the points of the IRC defining *phases IV*, *V*, *VII* and *VIII* involved in the formation of the O1−C5 and C3−O4 single bonds along the most favourable reactive channel associated with the *zw-type* 32CA reaction between nitrone **1b** and ketene **4b**. The electron populations, in e, are given in brackets.
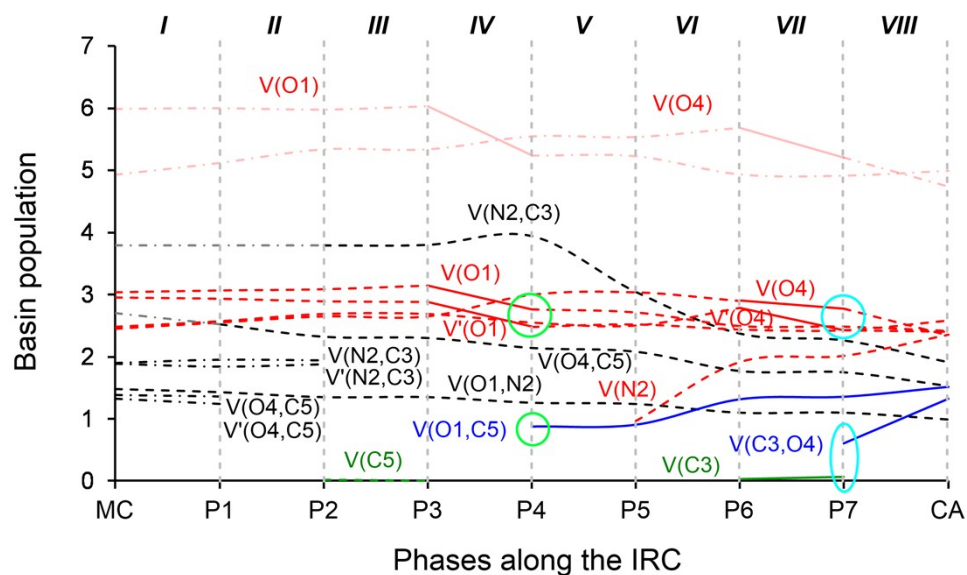
Figure S3. Graphical representation of the basin population changes along the *zw-type* 32CA reaction between nitrone **1b** and ketene **4b**. Dash dotted curves represent bonding regions described by two basins, dashed curves represent bonding regions described by only one basin and lined curves represent the basins directly involved in the formation of the new single bonds; black curves represent basins that do not participate in the bond formation processes, grey curves represent the sum of basins characterising a bonding region, the red colour is for lone pairs, green for *pseudoradical centers* and blue for the new formed single bonds.

*2. ELF topological analysis of the stationary points involved in the most favourable reactive channel associated with the 32CA reaction of nitrone **1b** with electrophilic ketene **4c**.*

In order to understand how the electron-withdrawing substitution in the ketene can modify the molecular mechanism of the *zw-type* 32CA reaction of nitrones with electrophilic ketenes, the bonding patterns of the stationary points involved in the most favourable reactive channel associated with the 32CA reaction of nitrone **1b** with electrophilic ketene **4c** were characterised by ELF topological analysis. The populations of the most significant valence basins are displayed in Table S3, while their associated attractor positions are represented in Figure S4.

At **MC-c**, d(O1−C5) = 2.647 Å and d(C3−C4) = 3.204 Å, the nitrone framework appears characterised by two monosynaptic basins, V(O1) and V'(O1), integrating a total population of 5.96e, one V(O1,N2) disynaptic basin integrating 1.48e and two disynaptic basins, V(N2,C3) and V'(N2,C3), with populations of 1.87e and 1.93e. These valence basins are related to the nitrone O1 oxygen lone pairs, and to the O1−N2 single and N2−C3 double bonds, respectively. On the other hand, the ketene framework is characterised by the presence of two monosynaptic basins, V(O4) and V'(O4), with a total population of 4.68e, associated with the ketene O4 oxygen lone pairs, two disynaptic basins, V(O4,C5) and V'(O4,C5), integrating a total of 3.00e, associated to the O4−C5 double bond, and two disynaptic basins, V(C5,C6) and V'(C5,C6), with a total of 4.13e associated to the C5−C6 double bond. The total population of the last pair of disynaptic basins remains *ca.* 4.1e along the reaction channel. At **MC-c**, there is no GEDT yet, 0.03e.

At **TS1-CO**, d(O1−C5) = 2.492 Å and d(C3−C4) = 3.180 Å, there are no significant topological changes with respect to the topological features of **MC-c**, only very slight electron population variations. This behaviour accounts for the very early character of **TS1-CO**, which has been previously deduced from the energy and geometry analysis of this TS. The GEDT at **TS1-CO** remains very low, 0.05e.

At **IN-CO**, d(O1−C5) = 1.569 Å and d(C3−C4) = 2.745 Å, the presence of a new V(O1,C5) disynaptic basin, integrating an electron population of 1.01e, indicates that the first O1−C5 single bond is already formed. In addition, the strong depopulation of the V(O1) and V'(O1) monosynaptic basins by 0.88e suggests that formation of the first

O1−C5 single bond has taken place through the donation of some electron density of the O1 oxygen lone pairs of the nitrone framework to the C5 carbon of the ketene one. This topological change requires the depopulation of the C5 carbon environment, which is evidenced by the decrease of the electron density present in the O4−C5 bonding region by 0.63e, in such a manner that at **IN-CO** only one V(O4,C5) disynaptic basin appears in this region, as well as by the increase of the total population of the V(O4) and V'(O4) monosynaptic basins by 0.69e. At **IN-CO**, the GEDT is very high, 0.45e, which accounts for the high polar character of this *zw-type* 32CA reaction.

At **TS2-CO**, d(O1−C5) = 1.479 Å and d(C3−C4) = 2.101 Å, while the two V(N2,C3) and V'(N2,C3) disynaptic basins present at **IN-CO** have merged into one V(N2,C3) disynaptic basin as a consequence of the strong depopulation of the N2−C3 bonding region by 0.89e, a new V(N2) monosynaptic basin, integrating 1.08e, is observed, which is associated with the N2 nitrogen lone pair present at the final CA **9c**. The population of the V(O1,N2) disynaptic basin has decreased to 1.21e. Interestingly, although the total population of the V(O4) and V'(O4) monosynaptic basins at **TS2-CO** is the same as at **IN-CO**, *ca.* 1e has been exchanged between them, in such a manner that the less populated V(O4) monosynaptic basin is perpendicularly disposed towards the nitrone C3 carbon. Note their different parallel orientation towards the nitrone framework in **P6** in Figure S2. At **TS2-CO**, the GEDT remains very high, 0.42e.

Finally, at **9c**, d(O1−C5) = 1.339 Å and d(C3−C4) = 1.436 Å, the presence of a V(C3,O4) disynaptic basin, integrating 1.33e, together with the presence of only one V(O4) monosynaptic basin after both, V(O4) and V'(O4), basins have been depopulated by 0.81e, justifies the formation of the second C3−O4 single bond at the end of the reaction path, apparently through the donation of some electron density of the O4 oxygen lone pairs to the C3 carbon. Accordingly, the V(N2,C3) disynaptic basin has decreased its population by 1e. The V(O1,N2), V(O4,C5) and V(O1,C5) disynaptic basins have low electron populations of 1.00e, 1.66e and 1.65e, while the V(N2) monosynaptic basin and those associated with the O1 oxygen atom have reached 2.34e and 4.78e. At **9c**, the GEDT is 0.19e.

Table S3. Valence basin populations N calculated from the ELF of the stationary points involved the most favourable reactive channel associated with the *zw-type* 32CA reaction between nitrone **1b** and ketene **4c**. Distances are given in Å, GEDT values and electron populations in e, and relative energies in kcal·mol⁻¹.

|	**MC-c**	**TS1-CO**	**IN-CO**	**TS2-CO**	**9c**
d(O1−C5)	2.647	2.492	1.568	1.479	1.339
d(C3−O4)	3.204	3.180	2.745	2.101	1.436
ΔE	0.0	−1.0	−6.4	−1.8	−23.7
GEDT	0.03	0.05	0.45	0.42	0.19
V(O1,N2)	1.48	1.44	1.29	1.21	1.00
V(N2)				1.08	2.34
V(N2,C3)	1.87	1.88	1.90	2.93	1.93
V'(N2,C3)	1.93	1.91	1.92		
V(O4,C5)	1.51	1.52	2.35	2.27	1.66
V'(O4,C5)	1.49	1.46			
V(O1)	2.91	2.93	2.50	2.46	2.26
V'(O1)	3.05	3.09	2.64	2.69	2.52
V(C5)					
V(C3)					
V(O4)	2.32	2.43	2.76	1.76	4.58
V'(O4)	2.36	2.27	2.63	3.63	
V(O1,C5)			1.01	1.05	1.65
V(C3,O4)					1.33
V(C5,C6)	2.05	2.08	2.09	2.04	1.99
V'(C5,C6)	2.08	2.03	1.94	2.01	2.00
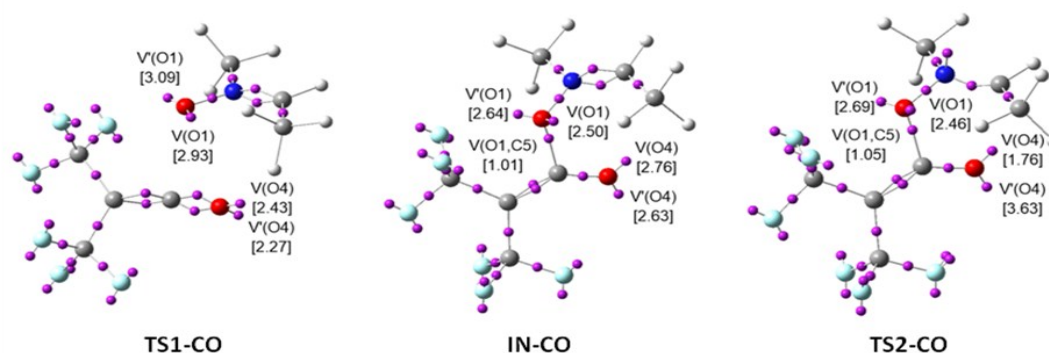
Figure S4. ELF attractor positions of the stationary points involved in the most favourable reactive channel associated with the *zw-type* 32CA reaction between nitrone **1b** and ketene **4c**. The electron populations, in e, are given in brackets.

References

1   X. Krokidis, S. Noury and B. Silvi, *J. Phys. Chem. A* 1997, **101**, 7277–7282.

2   (a) S. Berski, J. Andrés, B. Silvi and L. R. Domingo, *J. Phys. Chem. A*, 2003, **107**, 6014–6024; (b) V. Polo, J. Andrés, S. Berski, L. R. Domingo and B. Silvi, *J. Phys. Chem. A*, 2008, **112**, 7128–7136; (c) J. Andrés, P. Gonzáez-Navarrete and V. Safont, *Int. J. Quantum Chem.*, 2014, **114**, 1239–1252.

3   (a) R. Thom, *Structural Stability and Morphogenesis: An Outline of a General Theory of Models*, Inc.:Reading, MA, 1976; A. E. R. Woodcock and T. Poston, *A Geometrical Study of Elementary Catastrophes*, Spinger-Verlag, Berlin, 1974; (c) R. Gilmore, *Catastrophe Theory for Scientists and Engineers*, Dover: New York, 1981.

4   A. D. Becke and K. E. Edgecombe, *J. Chem. Phys.*, 1990, **92**, 5397–5403.

5   (a) V. Polo, J. Andrés, R. Castillo, S. Berski and B. Silvi, *Chem. Eur. J.*, 2004, **10**, 5165–5172; (b) J. C. Santos, J. Andrés, A. Aizman, P. Fuentealba and V. Polo, *J. Phys. Chem. A*, 2005, **109**, 3687–3693; (c) S. Berski, J. Andrés, B. Silvi and L. R. Domingo, *J. Phys. Chem. A*, 2006, **110**, 13939–13947; (e) V. Polo and J. Andrés, *J. Chem. Theory Comput.*, 2007, **3**, 816–823; (d) S. Berski, Z. Ciunik, *Mol. Phys.* 2015, **113**, 765–781.

6   M. Ríos-Gutiérrez, P. Pérez and L. R. Domingo, *RSC Advances*, 2015, **5**, 58464–58477.

7   L. R. Domingo, M. Ríos-Gutiérrez and J. A. Sáez, *RSC Advances* 2015, **5**, 37119–37129.

8   L. R. Domingo, J. A. Saéz, R. J. Zaragozá and M. Arnó, *J. Org. Chem.*, 2008, **73**, 8791–8799.

Table S4. MPWB1K/6-311G(d,p) total (E, in a.u.) and relative[a] (ΔE, in kcal·mol⁻¹) energies of the stationary points involved in the 32CA reactions between nitrone **1b** and ketenes **4b**,**c**.

	Gas Phase		Benzene	
	E	ΔE	E	ΔE
1b	-248.359809		-248.364325	
4b	-231.162850		-231.164119	
4c	-826.640748		-826.642094	
MC-b	-479.529336	-4.2	-479.533659	-3.3
TS-CO	-479.517467	3.3	-479.523646	3.0
TS-CC	-479.491986	19.2	-479.498757	18.6
9b	-479.568517	-28.8	-479.570891	-26.6
10b	-479.604187	-51.2	-479.608542	-50.3
MC-c	-1075.010424	-6.2	-1075.018724	-7.7
TS1-CO	-1075.011988	-7.2	-1075.016572	-6.4
IN-CO	-1075.020692	-12.6	-1075.032995	-16.7
IN-CC	-1075.011163	-6.7	-1075.021469	-9.4
TS-rot	-1075.007158	-4.1	-1075.017906	-7.2
TS2-CO	-1075.013288	-8.0	-1075.022860	-10.3
TS2-CC	-1075.000152	0.3	-1075.007664	-0.8
9c	-1075.048164	-29.9	-1075.052984	-29.2
10c	-1075.081751	-50.9	-1075.085491	-49.6

[a] Relative to the separated reagents **1b** + **4b** or **1b** + **4c**.

Table S5. MPWB1K/6-311G(d,p) enthalpies (H, in a.u.), entropies (S, in cal·mol⁻¹·K⁻¹) and Gibbs free energies (G, in au), and the relative[a] ones (ΔH in kcal·mol⁻¹, ΔS in cal·mol⁻¹·K⁻¹ and ΔG in kcal·mol⁻¹), computed at room temperature and 1 atm in benzene, for the stationary points involved in the 32CA reactions between nitrone **1b** and ketenes **4b,c**.

	H	ΔH	S	ΔS	G	ΔG
1b	-248.253197		74.0		-248.288369	
4b	-231.065563		75.7		-231.101508	
4b	-826.585676		97.2		-826.631874	
MC-b	-479.321378	-1.6	114.5	-56.7	-479.375786	8.8
TS-CO	-479.312717	3.8	102.1	-69.2	-479.361226	18.0
TS-CC	-479.288513	19.0	100.6	-70.6	-479.336319	33.6
9b	-479.357366	-24.2	100.9	-70.4	-479.405306	-9.7
10b	-479.394493	-47.5	98.0	-73.3	-479.441038	-32.1
MC-c	-1074.848956	-6.3	131.8	-39.4	-1074.911591	5.4
TS1-CO	-1074.847973	-5.7	128.9	-42.3	-1074.909222	6.9
IN-CO	-1074.862833	-15.0	126.0	-45.3	-1074.922697	-1.5
IN-CC	-1074.851142	-7.7	121.3	-50.0	-1074.908752	7.2
TS-rot	-1074.850383	-7.2	121.9	-49.3	-1074.908308	7.5
TS2-CO	-1074.853879	-9.4	121.8	-49.4	-1074.911760	5.3
TS2-CC	-1074.838885	0.0	120.0	-51.3	-1074.895897	15.3
9c	-1074.881602	-26.8	122.3	-49.0	-1074.939689	-12.2
10c	-1074.913346	-46.7	116.6	-54.7	-1074.968730	-30.4

[a] Relative to the separated reagents **1b** + **4b** or **1b** + **4c**.